PHYSICAL REVIEW D

PARTICLES AND FIELDS

THIRD SERIES, VOLUME 37, NUMBER 5 1 MARCH 1988

Nonsinglet valence-quark distribution from neutrino-deuterium deep-inelastic scattering

J. B. Cole,* S. Kunori, G. A. Snow, C. Y. Chang, and P. H. Steinberg†
University of Maryland, College Park, Maryland 20742

R. A. Burnstein, J. Hanlon,‡ and H. A. Rubin
Illinois Institute of Technology, Chicago, Illinois 60616

T. Kitagaki, S. Tanaka, H. Yuta, K. Abe, K. Hasegawa, A Yamaguchi, K. Tamai, Y. Otani, H. Hayano, H. Sagawa, and Y. Yanokura
Tohoku University, Sendai 980, Japan

T. Kafka, W. A. Mann, A. Napier, and J. Schneps
Tufts University, Medford, Massachusetts 02155
(Received 29 June 1987)

The deep-inelastic scattering reaction $\nu_\mu N \to \mu^- X$ has been studied using the deuterium-filled 15-foot bubble chamber at Fermilab. The data have been analyzed under the assumption of isospin invariance to extract $x(u_V - d_V)$ for the proton, where $xu_V(x)$ and $xd_V(x)$ are the valence up- and down-quark momentum distributions, respectively. The results are compared with other data and with different theoretical fits. The ratio $\nu n/\nu p$ as a function of x is also presented.

I. INTRODUCTION

Lepton-nucleon deep-inelastic scattering experiments are the source of many important insights into the quark structure of matter that now form the basis for the current theory of strong interactions, quantum chromodynamics (QCD). QCD cannot, however, predict structure functions or quark momentum distributions in even the simplest hadronic systems because of the importance of nonperturbative effects. Further progress in understanding the behavior of quarks in the nucleon and in the nucleus depends therefore, on accurate experimental data. Questions also remain about the range on which perturbative QCD calculations are valid.

Perhaps the simplest quark momentum distribution is that of the difference between the fractional momentum distributions of the valence u and d quarks in the proton, $xu_V(x) - xd_V(x)$, where x is the fraction of the proton's momentum carried by the quark. This quantity, often called the non(iso)singlet momentum distribution, is a useful object to study because it is independent of the quark singlet and gluon distributions in the Altarelli-Parisi equations for Q^2 evolution[1] and depends only weakly on $R = (F_2 - 2xF_1)/2xF_1$, which measures the violation of the Callan-Gross relation. The extraction of a singlet quark distribution always involves some assumption about R, the value of which is still not well understood.

To extract the nonsinglet quark distribution we studied the inclusive reaction $\nu_\mu N \to \mu^- X$ in the 15-foot deuterium-filled bubble chamber at Fermilab. The cross section is dominated by the process $\nu_\mu d \to \mu^- u$, but others such as $\nu_\mu \bar{u} \to \mu^- \bar{d}$ also contribute. If, however, the valence-quark distributions in the neutron and the proton obey isospin invariance and if their ocean-quark distributions are nearly the same, $x(u_V - d_V)$ can be extracted from the difference between the neutron and proton cross sections. Of course the deuteron is more than the sum of its nucleons, but it is only weakly bound, so that any corrections which might arise from pion exchange or six-quark structure effects can be neglected. We do, however, correct the event distributions for the effects of nucleon motion on the cross sections.

We distinguish νn and νp events by counting the total charge of the visible tracks in the final state. Since the neutrino flux is the same on both the neutrons and the protons, the extraction contains no relative uncertainty between different neutrino fluxes as in other kinds of experiments, but there is a systematic uncertainty due to "rescattering", in which a fraction of the νn events are misidentified as νp events. We determined the neutrino flux from the quasielastic reaction rate, $\nu_\mu n \to \mu^- p$, in the same experimental run[2] and used it to determine a total νD cross section that is very close to the current world average.[3]

In Sec. III we outline the analysis by which number distributions are obtained for νn and νp events in bins of x from the bubble-chamber data. In Sec. IV $x(u_V - d_V)$ is extracted from these distributions and from the neutrino flux and in Sec. V the results are compared with other experimental data and with various theoretical parametri- zations. We also discuss the ratio of the num-

ber of νn to νp events, which is relevant both to the determination of u_V/d_V and to the number of neutrino generations from the $Z^0/W^{\pm}$ cross-section ratio. We begin with a brief review of the parton model.

II. THE PARTON MODEL

Figure 1 defines the kinematics in the parton-model description of the dominant process in the νN charged-current interaction. An incoming neutrino with momentum $k=(E_\nu,\mathbf{k})$ emits a W^+ boson of momentum $q=k-k'$ which converts a d quark carrying a fraction x of the nucleon's momentum p into a u quark. The final state consists of an outgoing negative muon with momentum $k'=(E_\mu,\mathbf{k}')$ plus hadrons.

Experimentally one needs to determine only k and k' to compute any of the other variables of interest. In terms of $Q^2\equiv -q^2$ and $y\equiv(E_\nu-E_\mu)/E_\nu$, x is determined from $Q^2=2MxyE_\nu$, where M is the nucleon mass, and the muon mass is neglected.

The neutrino-nucleon charged-current cross sections can be written[4,5]

$$\frac{d^2\sigma^{\nu p}}{dx\,dy}=\frac{2xG_F^2ME_\nu}{\pi}[(d+s)+(1-y)^2(\bar{u}+\bar{c}) +\tfrac{1}{2}(1-y)q_L^{\nu p}] , \tag{1}$$

$$\frac{d^2\sigma^{\nu n}}{dx\,dy}=\frac{2xG_F^2ME_\nu}{\pi}[(u+s)+(1-y)^2(\bar{d}+\bar{c}) +\tfrac{1}{2}(1-y)q_L^{\nu n}] , \tag{2}$$

where each quark symbol stands for a function of x and Q^2. Under the assumption of isospin invariance $u^n=d^p\equiv d$, $d^n=u^p\equiv u$, $s^n=s^p\equiv s$, $c^n=c^p\equiv c$. The longitudinal quark distribution q_L is defined by $F_L=F_2-2xF_1\equiv xq_L$. Subtracting (1) from (2) we obtain

$$\frac{d^2\sigma^{\nu n-\nu p}}{dx\,dy}=\frac{2xG_F^2ME_\nu}{\pi}[(u_V-d_V) +\tfrac{1}{2}(1-y)(q_L^{\nu n}-q_L^{\nu p})] , \tag{3}$$

where $d^2\sigma^{\nu n-\nu p}/dx\,dy\equiv d^2\sigma^{\nu n}/dx\,dy-d^2\sigma^{\nu p}/dx\,dy$. We assume that $u_s=d_s=\bar{u}=\bar{d}$. The subscripts V and S denote the valence and ocean components of the quark distribution, respectively. See Ref. 6 for further discussion of this assumption.

As violations of the Callan-Gross relation affect the nonsinglet cross section (3) only through the difference term $q_L^{\nu n}-q_L^{\nu p}$, they are expected to nearly cancel except at low x, where soft-gluon emission is significant.

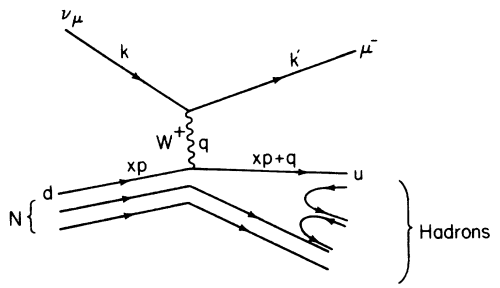

FIG. 1. Charged-current neutrino-nucleon scattering.

To first order in QCD $(q_L^{\nu n}-q_L^{\nu p})$ is given by[7]

$$(q_L^{\nu n}-q_L^{\nu p})\,|_{(x,Q^2)}=\frac{\alpha_S}{2\pi}x\int_x^1\frac{dz}{z^2}\frac{16}{3}(u_V-d_V)\Big|_{(z,Q^2)} , \tag{4}$$

where it is assumed that ocean distributions cancel in the integrand. Evaluating the integral with reasonable values for (u_V-d_V) and for α_S, we find that $(q_L^{\nu n}-q_L^{\nu p})$ makes its maximum contribution in the first x bin, where $(q_L^{\nu n}-q_L^{\nu p})<0.12(u_V-d_V)$. In this bin $\langle y\rangle=0.606$, so $\frac{1}{2}(1-y)(q_L^{\nu n}-q_L^{\nu p})<0.024(u_V-d_V)$. As x increases the relative size of the longitudinal contribution decreases rapidly.

We are thus left with the simple result

$$\frac{d^2\sigma^{\nu n-np}}{dx\,dy}\simeq\frac{G_F^2ME_\nu}{\pi}2x(u_V-d_V) . \tag{5}$$

This is the starting point for our extraction of $x(u_V-d_V)$ from the experimental data in Sec. IV.

III. EXPERIMENTAL PROCEDURE

The 15-foot bubble chamber at Fermilab was exposed to the wide-band neutrino beam produced by a total of 4.76×10^{18} 350-GeV protons incident on a beryllium oxide target. A 30-kG magnetic field was applied to the bubble chamber. We analyze the interactions in a 16.7-m^3 fiducial volume recorded on 320 000 sets of (three) photographic frames.

References 2 and 8–11 contain details of the experiment and of the primary analysis so we recount them only briefly.

A. Primary analysis

The photographs were examined for neutral-induced interactions. The particle tracks were measured and reconstructed using a computer fitting program which gave the momentum associated with each track. The first step was to identify the muon track using a kinematic method,[12] which incorporates the fact that the muon track tends to have a large-momentum component transverse ($P_{\rm Tr}^{\mu}$) to the total hadronic momentum. Events for which $P_{\rm Tr}^{\mu}<1.0$ GeV are rejected. The energies of the particles associated with the remaining tracks were calculated under the assumption that they had the pion mass, except when there were indications to the contrary. This source of error in the determination of E_ν was studied with a Monte Carlo program and is incorporated into the corrections described in Sec. III C. E_ν was determined using the method of Heilmann[13] in which momentum conservation in the directions longitudinal and transverse to the neutrino direction is applied, together with the assumption that the ratio of total longitudinal to total transverse momentum is the same for both charged and neutral hadrons. At best, this assumption is true only in a statistical sense, so it should be applied only to "reasonably" large event samples that have sufficient energy to produce many hadrons. For this reason we impose the acceptance cut $E_\nu>10$ GeV, and require that the total

TABLE I. The corrected number distributions.

			Neutron distribution			
bin	x range	N^e	N^n_{rs}	F_C	N^n	[a]
1	0.05–0.10	455	502	1.041	523	$\pm 27^{+21}_{-20}$
2	0.10–0.20	1280	1412	1.085	1532	$\pm 47^{+62}_{-57}$
3	0.20–0.30	1322	1460	1.102	1609	$\pm 49^{+65}_{-60}$
4	0.30–0.40	1089	1202	1.143	1374	$\pm 46^{+55}_{-51}$
5	0.40–0.50	778	858	1.206	1035	$\pm 41^{+42}_{-39}$
6	0.50–0.60	448	494	1.168	577	$\pm 30^{+23}_{-21}$
7	0.60–0.70	214	236	1.131	267	$\pm 20^{+11}_{-10}$
8	0.70–0.80	91	101	0.902	91	$\pm 10^{+3}_{-4}$
			Proton distribution			
bin	x range	N^o	N^p_{rs}	F_C	N^{pb}	
1	0.05–0.10	426	379	1.089	405	$\pm 27^{-21}_{+19}$
2	0.10–0.20	962	830	1.074	874	$\pm 36^{-60}_{+55}$
3	0.20–0.30	894	757	1.050	779	$\pm 32^{-60}_{+56}$
4	0.30–0.40	600	487	1.113	532	$\pm 24^{-53}_{+48}$
5	0.40–0.50	375	294	1.034	298	$\pm 16^{-35}_{+33}$
6	0.50–0.60	209	163	0.980	156	$\pm 11^{-19}_{+18}$
7	0.60–0.70	86	64	0.844	53	$\pm 6^{-8}_{+7}$
8	0.70–0.80	28	19	0.571	10	$\pm 2^{-2}_{+3}$
				N^n-N^p distribution		
bin	x range				N^{n-p}	
1	0.05–0.10				118	$\pm 38^{+43}_{-39}$
2	0.10–0.20				659	$\pm 59^{+121}_{-112}$
3	0.20–0.30				830	$\pm 58^{+125}_{-116}$
4	0.30–0.40				843	$\pm 52^{+108}_{-100}$
5	0.40–0.50				737	$\pm 44^{+79}_{-71}$
6	0.50–0.60				421	$\pm 32^{+42}_{-39}$
7	0.60–0.70				214	$\pm 21^{+19}_{-17}$
8	0.70–0.80				80	$\pm 11^{+6}_{-5}$

[a]First error is statistical, second is systematic corresponding to $f_{rs}=0.094\pm 0.035$.
[b]$N^p_{rs}F_C/1.02$ (corrected for nonisoscalarity).

visible longitudinal momentum be >5 GeV. We also introduce the acceptance condition $E_\nu<200$ GeV to eliminate spurious events.

Monte Carlo calculations indicate that 95.4% of the selected events are ν_μ charged-current events, the remainder being mostly neutral-current ν_μ events.

B. Selecting deep-inelastic events

Further conditions are now imposed to select deep-inelastic scattering events. The total hadronic mass W given by

$$W^2=(p+q)^2=M^2+Q^2\left[\frac{1}{x}-1\right]$$

is required to satisfy $W>2$ GeV in order to eliminate quasielastic reactions. Events with low-momentum transfer are excluded by the condition $Q^2>2$ GeV^2. Low-momentum muons that are difficult to resolve from the hadrons are eliminated by requiring $y<0.9$.

From this event sample we obtain the number distributions for even- and odd-pronged events in x bins 0.05–0.1, 0.1–0.2, . . . , 0.7–0.8. Events with $x<0.05$ events are excluded.

C. Correcting the distributions

To extract the true event distributions we must consider the following.

(1) Processing efficiency. The bubble-chamber photographs were visually scanned twice and the particle tracks were digitized. To correct for events that were not measurable or missed in the scanning, each event was given a prong-dependent weight which averaged 1.20. With this correction, the set of events which survive the acceptance cuts corresponds to 9794 νD events, of which 6002 are even-pronged (apparent νn events) and 3792 are odd-pronged (apparent νp events). The binned x distributions are displayed in Table I.

(2) Rescattering. From charge conservation, a νn (νp) event must produce an even (odd) number of charged tracks. For target neutrons bound in a deuteron, the proton that does not take part in the interaction (a "spectator" proton) follows the Hulthen momentum distribution which extends to values above 200 MeV thus some of the spectator protons have tracks long enough to be visible in the bubble chamber, and change the topology of a νn event (even prong) into that of an apparent νp event (odd prong). In addition it may happen that the struck neutron or one of its fragments strikes the spectator proton

to produce an extra charged track, thus decreasing the number of even-pronged events. In this study, we counted as a spectator proton any identifiable proton with momentum ≤ 340 MeV. This definition was motivated by studies of the momentum distribution of protons in our data sample, and agrees well with our previous analysis of Ref. 8. To obtain the true number of neutron- and proton-target events we introduce the rescattering coefficient $f_{\rm rs}$ as the fraction of neutron-target events that are odd-pronged. The number of (neutron-target) even-pronged events N^e is thus $N^e = N^n - f_{\rm rs} N^n$, whence $N^n = N^e/(1-f_{\rm rs})$. The number of proton events N^p is found by subtracting N^n from the total number of events. Table I shows N^n and N^p in each x bin. The value of $f_{\rm rs}$ is estimated[8] to be 0.094 ± 0.035 by extrapolating studies of the rescattering rates in proton-deuterium and pion deuterium interactions.

Proton rescattering onto a spectator neutron is also possible, but this does not affect the evenness or oddness of the track count.

(3) Monte Carlo corrections. Some of the data cuts that were introduced to select charged-current events may distort the "true" event distributions. Additional errors arise from the Fermi motion of the nucleons in the deuterium, from track measurement and reconstruction, and from contamination of the ν_μ charged-current-event sample by both ν_μ neutral-current events and $\bar{\nu}_\mu$ events. We correct the distributions for these effects with a Monte Carlo program that computes bin-by-bin correction factors.

The Monte Carlo (MC) program incorporates the following ingredients: (i) the measured energy distribution of beam neutrinos, and the antineutrino energy distribution in the beam from the Monte Carlo calculation of Ref. 14; (ii) input quark distributions that are used to generate both charged- and neutral-current νq and $\bar{\nu} q$ events; (iii) quark fragmentation using the Lund MC; (iv) Fermi motion of the target nucleon; (v) MARYB, a program that simulates the measurement process, including measurement errors and particle misidentification.

For a given number of MC events the ratio (F_C) of the bin contents of the input and output distributions from MARYB defines the MC correction factors. As column 5 of Table I shows, the corrections are typically about 10%. The Monte Carlo–corrected distributions are given in column 6 of the same table. The input quark momentum distributions[15] to the MC turned out to agree quite closely with our data so it was not necessary to refine the calculation of the MC correct factors by further iterations. The small differences that appear in the MC correction for neutron and proton events reflect the different shapes of the valence-quark distributions between the proton and neutron. In the kinematic region under study, $0.05 < x < 0.8$, the MC correction contributes only a small fraction of the observed neutron-proton difference. Moreover, the MC also successfully reproduces all the gross features of the hadrons observed in our ν_μ charged-current events.

(4) Nonisoscalarity. H_2 and HD contaminate the liquid deuterium in the bubble chamber giving it a 2% excess of protons over neutrons. This is corrected for by dividing the proton number distribution by 1.02. The numbers N^p in the sixth column of Table I incorporate this correction.

In summary, the results of this event selection and analysis procedure are the number distributions of events (see Table I) $\{N_i^n\}$, $\{N_i^p\}$, and $\{N_i^{n-p}\}$, where i denotes the ith x bin on the range $0.05 < x < 0.8$, subject to the acceptance conditions (i) $Q^2 > 2$ GeV, (ii) $W > 2$ GeV, (iii) $10 < E_\nu < 200$ GeV, and (iv) $y < 0.9$. We note that the x-bin averages of all kinematical variables (x, y, E_ν, Q^2, etc.) are very nearly the same for even-prong (neutron-target) and odd-prong (mostly proton-target) events. We have neglected radiative corrections which have been shown to be small.[16]

IV. EXTRACTION OF $x(u_V - d_V)$

Using Eq. (5) the difference of the numbers between n- and p-target interactions in the ith x bin is

$$N_i^{n-p} = (\rho V)\left[\frac{G_F^2 M}{\pi}\right]\int_{x_i^-}^{x_i^+} dx \int dE_\nu \int dy\, E_\nu \frac{d\phi(E_\nu)}{dE_\nu} \times 2x(u_V - d_V)\,, \tag{6}$$

where $d\phi(E_\nu)/dE_\nu$ (ν's/GeV cm^2) is the measured neutrino flux, V is the bubble-chamber fiducial volume, ρ is the number density of nucleons, and x_i^+ and x_i^- are the bin boundaries. The y and E_ν integration limits are determined by the conditions listed at the end of the last section.

The unknown function of x and Q^2, $x(u_V - d_V)$, is extracted by assuming (following QCD) only slow dependence on Q^2, and sufficiently small x dependence within the x bins so that it can be removed from the integral in (6). We obtain

$$N_i^{n-p} = K J_i x(u_V - d_V)\big|_{\bar{x}_i, \bar{Q}_i^2}\,, \tag{7}$$

where

$$J_i = \int_{x_i^-}^{x_i^+} dx \int dE_\nu \int dy\, E_\nu \frac{d\phi(E_\nu)}{dE_\nu}, \quad K = 2\rho V \frac{G_F^2 M}{\pi}\,,$$

and $\bar{x}_i$ and $\bar{Q}_i^2$ are the ith x bin averages of x and Q^2, respectively, as determined from the data. The $\bar{x}_i$ are close, but not necessarily equal to, the bin midpoints, x_i.

Using a functional fit to the neutrino flux, the integrals J_i are evaluated analytically, with care taken to respect all the constraints on the region of integration. The values of $x(u_V - d_V)$ at $(\bar{x}_i, \bar{Q}_i^2)$ obtained in this way are displayed in Table II.

Integrals of the form

$$K_i[f] = \int_{x_i^-}^{x_i^+} dx \int dE_\nu \int dy\, E_\nu \frac{d\phi(E_\nu)}{dE_\nu} f(x, y, E_\nu),$$

with the same constraints as in (6) and (7), where f is an arbitrary function of x, y, E_ν, can be used to predict the bin average of f knowing only the shape of the neutrino flux (normalization factors divide out). For example, taking $f = x$, we have

TABLE II. Unadjusted values of $x(u_V-d_V)$.

x range	$\bar{x}_{\rm bin}$	$\bar{Q}^2_{\rm bin}$ (GeV^2)	$x(u_V-d_V)$	[a]
0.05–0.10	0.077	5.9	0.168	$\pm0.055^{+0.060}_{-0.056}$
0.10–0.20	0.151	8.5	0.297	$\pm0.027^{+0.054}_{-0.051}$
0.20–0.30	0.246	11.7	0.316	$\pm0.022^{+0.048}_{-0.044}$
0.30–0.40	0.347	14.5	0.302	$\pm0.019^{+0.038}_{-0.036}$
0.40–0.50	0.444	18.3	0.263	$\pm0.016^{+0.028}_{-0.025}$
0.50–0.60	0.545	20.8	0.155	$\pm0.012^{+0.016}_{-0.014}$
0.60–0.70	0.642	27.7	0.084	$\pm0.008^{+0.007}_{-0.007}$
0.70–0.80	0.746	31.1	0.035	$\pm0.005^{+0.002}_{-0.003}$

[a]First error is statistical, second is systematic corresponding to $f_{\rm rs}=0.094\pm0.035$.

$$\bar{x}_i=\frac{K_i[x]}{J_i}\ .$$

Setting $f=x$, y, and E_ν we calculated the bin averages of these quantities and compared them with those found directly from the data on an event-by-event basis. Excellent agreement is obtained[11] suggesting that we have the correct flux shape and that our method of event reconstruction is reliable.

We studied the size of the term (4) in (3) using the Glück, Hoffmann, and Reya[15] (GHR) parametrizations for quark distributions, which turned out to be in good agreement with our data. These same parametrizations were also used in the Monte Carlo program to compute the corrections discussed in Sec. III C. The resultant (downward) correction to $x(u_V-d_V)$ is found to be about 2% in the first x bin and declines steadily with increasing x. It is not incorporated into our quoted results.

Finally we adjust our results to the bin centers and to a common Q^2 value, Q_s^2, by multiplying the $x(u_V-d_V)|_{\bar{x}_i,\bar{Q}_i^2}$ by the factors

$$a_i=\frac{x(u_V-d_V)_{\rm fit}|_{x_i,Q_S^2}}{x(u_V-d_V)_{\rm fit}|_{\bar{x}_i,\bar{Q}_i^2}}\ ,$$

where $x(u_V-d_V)_{\rm fit}$ is a theoretical or phenomenological parametrization. We used the GHR parametrization. For comparison with other published data we quote our results at $Q_S^2=11.0$ and 15.0 GeV^2 (Table III). The adjustments average 3% or less for the first five bins and are always less than the statistical uncertainty. Overall, the Q^2 average of our data is about 12.0 GeV^2.

TABLE III. $x(u_V-d_V)$ at bin centers and common Q^2. Errors approximately the same as in Table II.

x	$Q^2=11$ GeV^2 $x(u_V-d_V)$	$Q^2=15$ GeV^2 $x(u_V-d_V)$
0.075	0.170	0.171
0.150	0.296	0.296
0.250	0.317	0.313
0.350	0.308	0.300
0.450	0.276	0.265
0.550	0.170	0.160
0.650	0.098	0.091
0.750	0.045	0.041

We report both our adjusted and unadjusted results, as well as the number distributions before rescattering corrections.

V. RESULTS AND CONCLUSIONS

Tables II and III and Fig. 2 display the results of our analysis. The figure plots $x(u_V-d_V)$ for both our standard value of the scattering fraction ($f_{\rm rs}$), and its upper and lower limits. Since the uncertainty in $f_{\rm rs}$ dominates the statistical uncertainty in most of the x range, much could be gained by reducing the uncertainty in $f_{\rm rs}$. There is also a systematic error in the neutrino flux determination, but since the total νD cross section that we determine from this flux is very close to the world average, we do not include it with the much larger systematic error in $f_{\rm rs}$.

We compare our results with data from the CERN-Dortmund-Heidelberg-Saclay[5] (CDHS), WA25[17] (BEBC), European Muon Collaboration[18] (EMC), and SLAC[19] experiments and with the parametrizations due to Glück, Hoffmann, and Reya[15] (GHR), Duke and Owens[20] (DO), and Abbott, Atwood, and Barnett[21] (AAB) in Figs. 3 and 4. Since AAB is an excellent description of most SLAC data we use it instead of the actual SLAC data in our comparisons.

When comparing our data with other results, it should

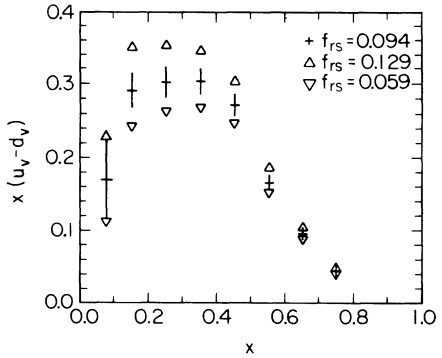

FIG. 2. $x(u_V-d_V)$ vs z at $Q^2=11$ GeV^2, for the central value of the rescattering coefficient, $f_{\rm rs}=0.094$ (+), and for its extreme values, $f_{\rm rs}=0.129$, (△) and $f_{\rm rs}=0.059$ (▽). The error bars represent the statistical errors.

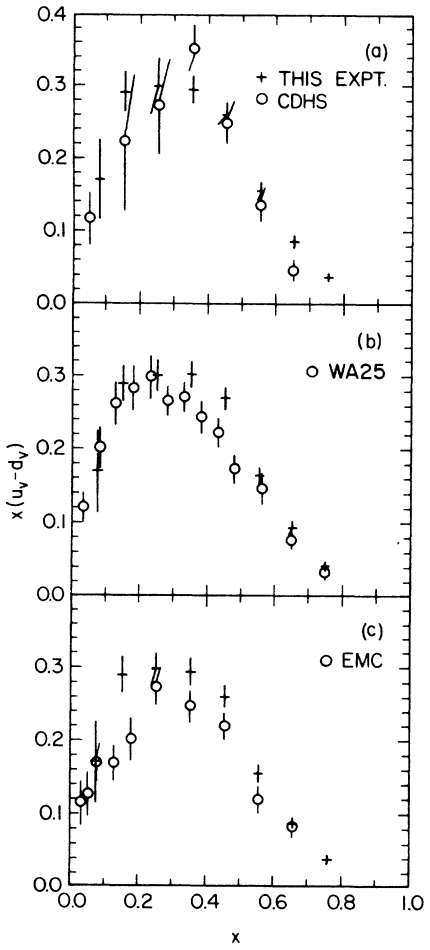

FIG. 3. (a) $x(u_V-d_V)$ vs x at $Q^2=15$ GeV^2. +, this experiment; ○ CDHS (Ref. 5). (b) $x(u_V-d_V)$ vs x at variable Q^2. +, this experiment (see Table II); ○, WA25 (Ref. 17). (c) $x(u_V-d_V)$ vs x. +, this experiment at $Q^2=15.0$ GeV^2; ○, EMC (Ref. 18) at variable Q^2.

be kept in mind that none of the above experiments determines $x(u_V-d_V)$ in the same manner as we do. They all derive the nonsinglet structure function by subtracting two singlet structure functions, obtained in different experimental runs. The CDHS Collaboration compares νp with $\bar{\nu}p$ interactions, while EMC studies the μ^+p and μ^+D reactions, and SLAC the eD and ep reactions.

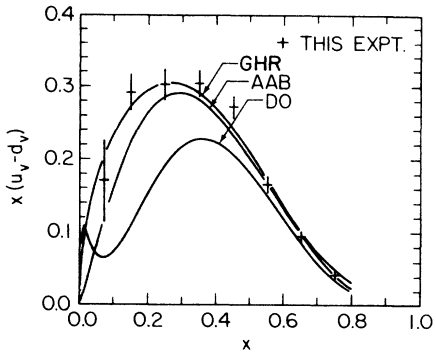

FIG. 4. $x(u_V-d_V)$ vs x at $Q^2=11$ GeV^2. The solid lines represent parametrizations of GHR (Ref. 15), AAB (Ref. 21), and DO (Ref. 20) set 2. AAB represents the best fit to SLAC data.

WA25 analyze the νD and $\bar{\nu}$D interactions in a bubble chamber and determine the structure functions F_2 and F_3 separately for νn and νp events, whence they deduce $x(u_V-d_V)$. As Fig. 3(b) shows, our results agree well with WA25 but, it should be noted that the two experimental analyses used somewhat different input parameters. WA25 takes f_{rs} to be 0.12, whereas we use 0.094, but the WA25 average νN cross section is 8% lower than ours so the differences happen to approximately cancel in the final result. The WA25 value for f_{rs} applied to our data would yield an estimate for the integral in (8) that is larger than the quark-parton model prediction. In the low-x region our results are higher than SLAC (AAB) and EMC.

Our results are reasonably well described by the GHR parametrization. Another due to Eichten, Hinchliffe, Lane, and Quigg[22] (EHLQ) also agrees fairly well. DO fit EMC and SLAC data, while maintaining the sum rule (8). This causes an "oscillation" (Fig. 4), because of the different rates at which $x(u_V+d_V)$ and xd_V vanish.

DO, EHLQ, and GHR all assume Altarelli-Parisi[1] Q^2 evolution and consistency with the Adler sum rule[23]

$$I\equiv\int_0^1 dx(u_V-d_V)=1 \tag{8}$$

in accord with the quark-parton model. AAB, on the other hand, drop these assumptions in their fit to SLAC data and incorporate "higher-twist" $(1/Q^2)$ terms to account for all of the Q^2 evolution, with no fixed normaliza-

TABLE IV. Values of $\int dx(u_V-d_V)$. All integrals at $Q^2=11.0$ GeV^2 except where noted.

Fit/data set	Integration range 0–0.05[a]	0.05–1.0	0–1
This Expt.[b]	$0.34^{+0.06}_{-0.06}$	$0.64\pm0.03^{+0.12}_{-0.11}$	$0.98\pm0.03^{+0.18}_{-0.17}$
WA25			$1.01\pm0.08\pm0.18$
EMC ($Q^2=15$ GeV^2)			$0.72\pm0.06\pm0.39$
GHR	0.337	0.663	1
AAB	0.074	0.535	0.610
DO	0.621	0.379	1

[a]Calculated from a fit to data.
[b]Systematic errors refer to $f_{rs}=0.094\pm0.035$.

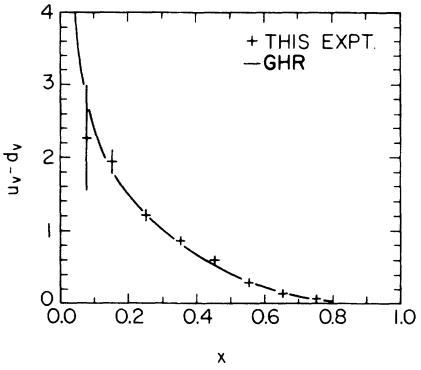

FIG. 5. $u_V - d_V$ vs x at $Q^2 = 11$ GeV^2. Solid line is GHR parametrization.

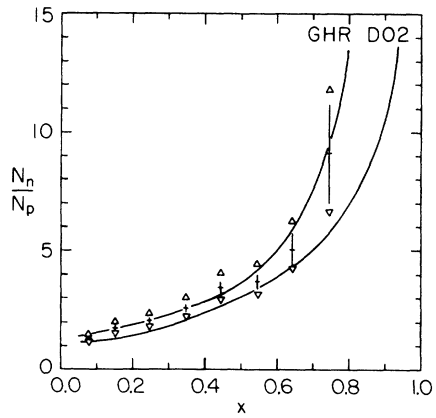

FIG. 6. Ratio of charged current νn to νp events as a function of x. Vertical bars indicate statistical errors and triangles depict upper and lower systematic error limits due to rescattering. Curves give the predictions of GHR (Ref. 15) and DO (ref. 20).

tion. The EMC (Ref. 24) also finds evidence for higher-twist terms in proton structure functions extracted from muon-proton scattering data that are resolvable up to $Q^2 = 20$ GeV^2. Such terms are thought to arise from nonperturbative QCD effects. How fast nonperturbative effects vanish as Q^2 increases is an important question that has yet to be answered definitively. Recent high-energy polarized scattering data indicate that nonperturbative effects may play a role at higher Q^2 than previously thought.[25]

To test the Adler sum rule we tried to estimate the value I. From our data in the range $0.05 < x < 1.0$ we estimated the integral of $u_V - d_V$ with respect to x to be $0.64 \pm 0.03^{+0.12}_{-0.11}$ (integral negligible for $0.8 < x < 1.0$). A one-parameter least-squares fit to the form $I(u_V - d_V)|_{\mathrm{GHR}}$ yielded $I = 0.98 \pm 0.03^{+0.18}_{-0.17}$. The first uncertainty is statistical, while the second reflects the rescattering uncertainty. This fit to the GHR form, shown in Fig. 5, has a confidence level of 5%. Table IV compares determinations of I from different experiments and parametrizations.

It has been pointed out by Halzen and Scott[26] that the ratio of the Z^0 and $W^{\pm}$ production cross sections in $p\bar{p}$ collisions can be used to set a limit on the number of neutrino generations if the ratio $u(x)/d(x)$ is known in the x and Q^2 region pertinent to the experiment in which $W^{\pm}$ and Z^0 cross sections are measured. The UA1 (Ref. 27) and UA2 (Ref. 28) collaborations have carried out such analyses using the structure functions given by GHR (Ref. 15) and DO (Ref. 20) and the QCD production cross sections for $W^{\pm}$ and Z^0 given by Altarelli *et al.*[29] As has been recently emphasized by Martin, Roberts, and Stirling,[30] the DO and GHR structure functions differ sufficiently to change the limit on the number of neutrino generations by about two. It is therefore of interest to compare their predictions for the N^n/N^p ratio with our data.

From Eqs. (1) and (2) it follows that

$$\frac{N^n}{N^p} = \frac{u_V + \frac{4}{3}\bar{u} + s}{d_V + \frac{4}{3}\bar{u} + s} \xrightarrow[x \gtrsim 0.2]{} \frac{u_V}{d_V} . \tag{9}$$

Figure 6 displays the comparison at $Q^2 = 11$ GeV^2 between GHR and DO (set 2 barely distinguishable from set 1). Our data clearly favor GHR over DO at $x \simeq 0.15$, which is the region most relevant to W and Z^0 production at the CERN collider, thus implying a higher limit on the number of neutrino families.[30]

Since our largest experimental uncertainty is in the rescattering fraction we attempted to form another estimate of its size. Recent data due to Aderholtz *et al.*[31] on the ratio $\sigma^{\nu n}/\sigma^{I=0}$ implies that $\sigma^{\nu n}/\sigma^{\nu p} = 2.05 \pm 0.08$ in excellent agreement with our earlier determination of $2.03 \pm 0.08 \pm 0.27$ (Ref. 8). Turning the argument around and combining the ratio of Aderholtz *et al.* for $\sigma^{\nu n}/\sigma^{\nu p}$ with our value of N^e/N^o (total number of even- and odd-prong events, respectively) gives $f_{\mathrm{rs}} = 0.098 \pm 0.019$ as compared with $f_{\mathrm{rs}} = 0.094 \pm 0.035$ which we use in this paper. One must be cautious, however, because neon and deuterium data are combined in this line of reasoning. It nevertheless does suggest that the systematic errors depicted in Figs. 3 and 6 are overestimated.

To summarize, we have extracted the nonsinglet nucleon quark momentum distribution from νD bubble-chamber data with an average Q^2 of 12 GeV^2. Our results are free of the relative systematic errors that are implicit in subtracting cross sections from different experimental runs, but they contain a systematic uncertainty due to rescattering. Our results are in good agreement with the Adler sum rule. Our data also provide information on the ratio $u(x)/d(x)$, which is relevant to the determination of a limit on the number of neutrino generations from the Z^0 to $W^{\pm}$ production ratio in $p\bar{p}$ collisions.

ACKNOWLEDGMENTS

We are indebted to the Fermilab accelerator and neutrino groups, to our scanning staffs, and to Professor R. Engelmann and the Stony Brook group who originally participated in this collaboration, as well as to Dr. D. Son and Dr. D. Zieminska. This research was supported by the United States Department of Energy, the National Science Foundation, and by the University of Maryland General Research Board and was assisted by the University of Maryland Computer Science Center.

*Present address: NASA, Goddard Space Flight Center, Code 661, Greenbelt, MD 20771.
†Deceased.
‡Present address: Fermi National Accelerator Laboratory, Batavia, Illinois 60510.

[1]M. Diemoz, F. Ferroni, and E. Longo, Phys. Rep. **130**, 293 (1986); G. Altarelli, *ibid.* **81**, 1 (1982).
[2]T. Kitagaki *et al.* Phys. Rev. Lett. **49**, 98 (1982); Phys. Rev. D **28**, 436 (1983).
[3]J. Feltesse, in *Proceedings of the International Europhysics Conference on High Energy Physics,* Bari, Italy, 1985, edited by L. Nitti and G. Preparata (Laterza, Bari, 1985), p. 979.
[4]T.-P. Cheng and L.-F. Li, *Gauge Theory of Elementary Particle Physics* (Oxford University Press, Oxford, England, 1984); C. Quigg, *Gauge Theories of the Strong, Weak, and Electromagnetic Interactions* (Benjamin/Cummings, Reading, MA 1983); F. E. Close, *An Introduction to Quarks and Partons* (Academic, New York, 1982).
[5]H. Abramowicz *et al.*, Z. Phys. C **25**, 29 (1984).
[6]D. A. Ross and C. T. Sachrajda, Nucl. Phys. **B149**, 497 (1979).
[7]A. J. Buras, Rev. Mod. Phys. **52**, 199 (1980). We apply Eq. (8.87).
[8]J. Hanlon *et al.*, Phys. Rev. Lett. **45**, 1817 (1980) (our earlier $\sigma^{\nu n}/\sigma^{\nu p}$ measurement using one-third of our present data set); in *Proceedings of the International Conference on Neutrinos, Weak Interactions and Cosmology,* Bergen, Norway, 1979, edited by A. Haatuft and C. Jarlskog (Fisik Institute, Bergen, 1980), Vol. II, p. 286.
[9]T. Kitagaki *et al.*, Phys. Lett. **97B**, 325 (1980); T. Kitagaki, in *Proceedings of the International Conference on Neutrino Physics and Astrophysics,* Maui, 1981, edited by R. J. Cence, E. Ma, and A. Roberts (Maui, Hawaii, 1985), Vol. II, p. 97.
[10]D. Zieminska *et al.*, Phys. Rev. D **27**, 47 (1983).
[11]J. B. Cole, Ph.D. thesis, University of Maryland, 1987.
[12]J. Bell *et al.*, Phys. Rev. D **19**, 1 (1979).
[13]H. G. Heilmann, Bonn Internal Report No. WA21-int 1, 1978 (unpublished); J. Blietschau *et al.*, Phys. Lett. **87B**, 281 (1979).
[14]S. Mori, Fermilab Report No. TM-663, 1976 (unpublished) and Report No. TM-720, 1977 (unpublished); J. Grimson and S. Mori, Fermilab Report No. TM-824, 1978 (unpublished).
[15]M. Glück, E. Hoffmann, and E. Reya, Z. Phys. C **13**, 119 (1982).
[16]R. Barlow and S. Wolfram, Phys. Rev. D **20**, 2198 (1979); D. Allasia *et al.*, Phys. Lett. **107B**, 148 (1981).
[17]D. Allasia *et al.*, Phys. Lett. **135B**, 231 (1984) [source for Fig. 3(b) data]. Other data appear in D. Allasia *et al.*, Z. Phys. C **28**, 321 (1985).
[18]J. J. Aubert *et al.*, Phys. Lett. **123B**, 123 (1983) [source for Fig. 3(c) data].
[19]Particle Data Group, C. G. Wohl *et al.*, Rev. Mod. Phys. **56**, S61 (1984); A. Bodek *et al.*, Phys. Rev. D **23**, 1070 (1981); **20**, 1471 (1979).
[20]D. W. Duke and J. F. Owens, Phys. Rev. D **30**, 49 (1984).
[21]L. F. Abbott, W. B. Atwood, and R. M. Barnett, Phys. Rev. D **22**, 582 (1980) [Eq. (3.18) multiplied by 3 to correct an apparent error or misprint].
[22]E. Eichten, I. Hinchliffe, K. Lane, and C. Quigg, Rev. Mod. Phys. **56**, 579 (1984) [Eq. (2.55)].
[23]S. L. Adler, Phys. Rev. **143**, 1144 (1966).
[24]J. J. Aubert *et al.*, Nucl. Phys. **B259**, 189 (1985).
[25]Physics Today **38**, (1)17 (1985).
[26]F. Halzen and D. M. Scott, Phys. Lett. **78B**, 318 (1978).
[27]G. Arnison *et al.*, Phys. Lett. B **185**, 241 (1987); **191**, 463 (1987).
[28]R. Ansari *et al.*, Phys. Lett. B **194**, 158 (1987).
[29]G. Altarelli *et al.*, Nucl. Phys. **B246**, 12 (1984); Z. Phys. C **27**, 617 (1985).
[30]A. D. Martin, R. G. Roberts, and W. J. Stirling, Phys. Lett. B **189**, 220 (1987).
[31]M. Aderholtz *et al.* Phys. Lett. B **173**, 211 (1986).